論文の内容の要旨

Ab initio theoretical study of high-harmonic generation from transition metal elements

(第一原理計算による遷移金属元素からの高次高調波発生の理論的研究)

ワーユータマ　イマム　セティアワン

When an intense laser field interacts with matter, one of the possible outcomes is the emission of a secondary radiation whose frequencies are multiples of the the primary radiation frequency. This electromagnetic process, which is referred to as high-harmonic generation (HHG), is in fact the most important outcomes of a strong-field interaction. Compared to the other common strong-field processes such as multiphoton ionization (MPI), tunneling-ionization, and non-sequential double ionization (NSDI), HHG is the closest to practical applications, whether for fundamental researches or commercial products.

HHG is classified as an extreme nonlinear process because it involves generation of harmonics up to tens, and sometimes hundreds, multiple of the fundamental frequency depending on laser intensity, wavelength, and atomic species. The fact that even a few hundreds of harmonic can be reached asserts that conventional nonlinear optics description will not suffice in explaining the phenomenon. To give numerical figures, the ionization energy of Ar gases from which HHG is usually generated is about 15.8 eV, hence for a driving laser at 800 nm there could only be about 10 photons absorbed to make the first ionization happen, implying that the harmonic train in the spectrum should terminate at around the tenth order, instead of more than a hundred as reported in some works. These observations strongly suggest that we need to set aside the perturbative nonlinear optics theory and devise a new model.

The most frequently used atomic elements to generate high harmonic radiations are rare gas atoms because they are readily available in gas phase and furthermore, their inert nature makes them easy to store. Other stable elements occuring naturally in gas phase like nitrogen is also used as HH source thanks to its high ionization potential, ~ 14.5 eV. In 2006, however, a group of researchers had a different idea in what they should use as the HH source. In particular, they created plasma plumes from metallic elements through laser ablation technique. Using a 796 nm laser whose intensity is on the order of 10^{14} W/cm^2 to generate HH from indium (Z = 49) plasma, they discovered that the HH spectrum exhibited a strong enhancement of the 13-th harmonic (20.3 eV) of the fundamental laser (see the red line in Fig. 1(a)) [1]. This peak is enhanced more than hundred times stronger than the neighboring ones.

Chromium (Z = 24) and manganese (Z = 25) plasmas are among the first transition metals physicists had observed an enhanced peak in the HH spectrum. The experimental HH spectra from chromium and manganese plasmas obtained using 800 nm driving laser are depicted in Fig. 1(b) and (c), where the enhancements are seen at the 29th (~ 45 eV) and 31st (~ 50 eV) harmonic order, respectively [2, 3]. The origin of this harmonic enhancement has been linked to a resonant emission with a giant transition line

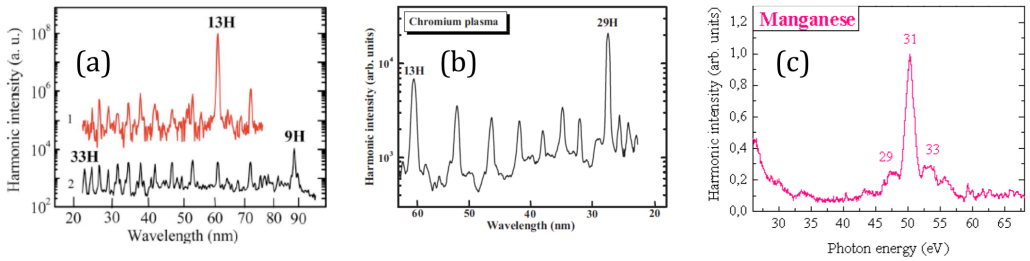

Figure 1: Experimental HH spectra from (a) In (red) and Ag (black) plasmas [Ganeev et al., *Opt. Lett.* **31**, 1699 (2006)], (b) Cr plasma [Ganeev et al., *Phys. Rev. A* **75**, 063806 (2007)], and (c) Mn plasma [Ganeev et al., *Opt. Express* **20**, 25239 (2012)].

present in the excitation spectrum of the plasma element. Some open questions which we address in this dissertation are first, which transition line is actually responsible for the resonance, which ionic species is the dominant source of enhancement, and ultimately, how this transition line manifests its presence in the high-harmonic spectrum. Aimed at answering these questions, in this work we attempt to approach the problems by means of theoretical methods that take into account all electrons present in the atom and solve the time-dependent wavefunction right from the exact Schrödinger equation.

The problem at hand, namely HHG from transition metal, demands a method which can properly treat multiple electrons at once during an interaction with laser field because these elements have multiple loosely bound electrons (typical ionization potential for transition metals is ~ 6 eV). A promising class of methods to investigate intense laser-driven multielectron dynamics in such systems is the *time-dependent multiconfiguration self-consistent-field* (TD-MCSCF) method, which describes the system wavefunction by a superposition of time-dependent Slater determinants. TD-MCSCF is a general denomination for first-principles methods which obtain the time-dependent orbitals and CI coefficients variationally. In this dissertation, we employ two extensions of TD-MCSCF, namely *time-dependent complete active space self-consistent field* (TD-CASSCF) [4, 5] and *time-dependent occupation restricted multiple active space* (TD-ORMAS) [6], in order to calculate the HH spectra and to perform the subsequent analyses. In TD-CASSCF and TD-ORMAS, one can set some orbitals to always be doubly occupied and be fixed in time. These orbitals are referred to as *frozen cores*. Other orbitals having arbitrary occupation between zero and two and are time-dependent are called *active orbitals*. A particular case of TD-CASSCF where all orbitals are active is conventionally called *multiconfiguration time-dependent Hartree-Fock* (MCTDHF) method. In the present work, these methods are extended to enable calculations of general open-shell atoms such as transition metals, having a number of unpaired valence electrons which can equally participate in the dynamics under strong laser fields. In performing the analyses, we take full advantage of TD-CASSCF and TD-ORMAS as a multiorbital method by studying the dynamics emerging in and between these orbitals [7]. The analyses employed in this dissertation are set up by emphasizing the response of these orbitals to a laser field with the aim to reveal the physics underpinning resonant HHG in a conventional and straightforward way.

First, we perform numerical simulations on Mn and Mn^+ by varying the boundary between frozen and active orbitals. The employed orbital subspace decompositions for Mn and Mn^+ are presented in Fig. 2(c) and (d), respectively. Setting the laser parameters at intensity of 3×10^{14} W/cm^2, center wavelength 770 nm, and 4-cycle pulse duration, we run MCTDHF simulations where all orbitals are active in Fig. 2(c) and (d) and the thick dark green spectra (denoted by MCTDHF in Fig. 2(a) and (b)) resulted. As it should be, this method, which is the most accurate simulation within 15 orbitals restriction, is able to seamlessly produce the resonant enhancement at 51.5 eV. Then, freezing up to $2p$ orbitals (using fz. $2p$ orbital decomposition in Fig. 2(c) and (d)), we obtain the thin cyan spectra which are practically still identical to the MCTDHF spectra in all ionic species. This result demonstrates that TD-CASSCF can be as accurate as MCTDHF provided the choice of orbital subspace decomposition is appropriate with respect to laser parameters. Adding one more orbital $3s$ to be frozen (using fz. $3s$ in Fig. 2(c) and (d)), we get the dashed yellow spectra (marked as fz. $3s$) exhibiting no discernible differences with previous two spectra. Finally, when $3p$ orbitals are frozen (using fz. $3p$ in Fig. 2(c) and (d)), a notable modification

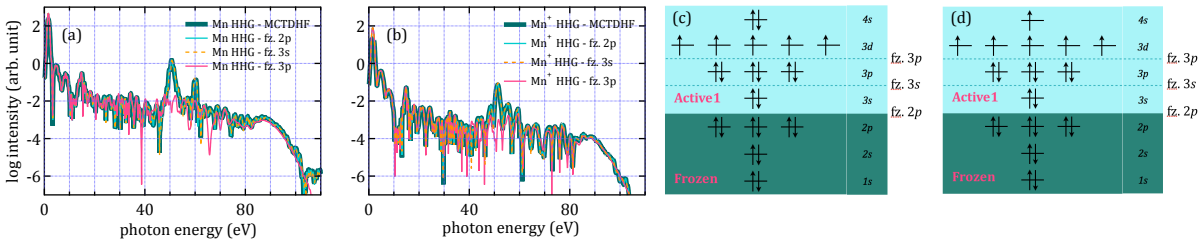

Figure 2: HH spectra from (a) Mn and (b) Mn^+ obtained using TD-CASSCF with orbital subspace decompositions differing in the boundary of the frozen set, see (c) for Mn and (d) for Mn^+. The laser intensity is 3×10^{14} W/cm^2 and the wavelength is 770 nm.

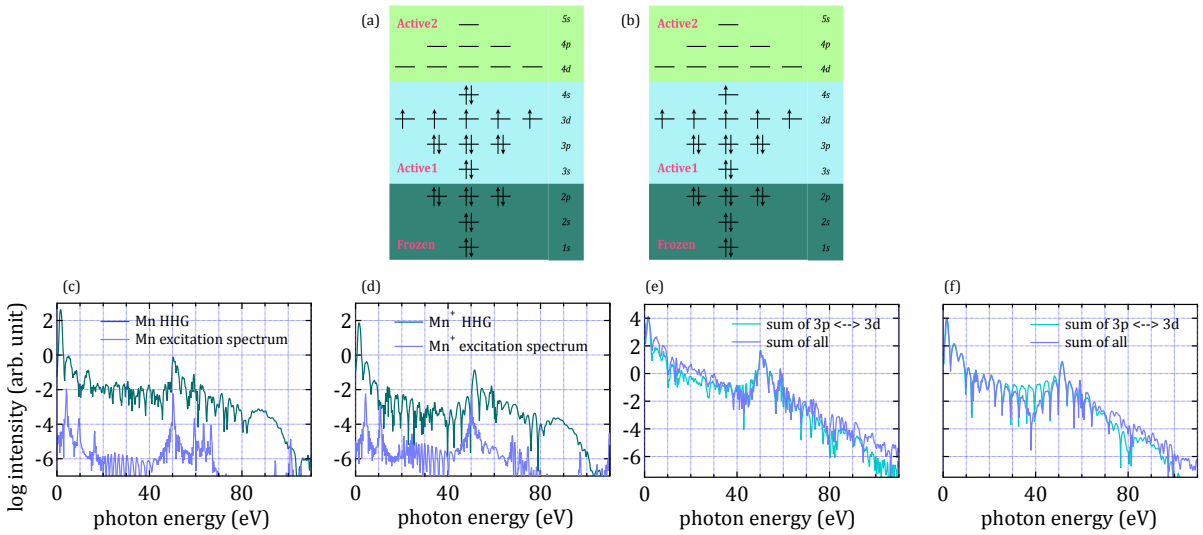

Figure 3: TD-ORMAS orbital subspace decompositions for (a) Mn and (b) Mn^+. The HH spectra are plotted in dark green in (c) and (d) along with the excitation spectra (purple). The total spectrum of $3p \leftrightarrow 3d$ transitions (cyan) and of all dipole-allowed transitions (purple) are depicted in (e) for Mn and (f) for Mn^+.

in the spectrum around the resonant energy is observed - the enhancement is lost. This observation hints at a crucial involvement of transitions from $3p$ orbitals in the enhancement process in Mn plasma because by freezing $3p$ orbitals, we are actually removing any determinants in the determinant basis set where $3p$ orbitals are not doubly occupied, i.e., no $3p$ transitions can happen if these orbitals are frozen. Fig. 2(a) and (b) further tells us that the contribution from these unknown transitions involving $3p$ is effectively limited to the enhancement only. If one compares fz. $3p$ spectra and any of the other three spectra in each ionic species, one sees that the differences in the shape of the peaks are remarkably small outside the enhancement region.

In the next analysis, we will decompose the HH spectra into contribution from orbital-orbital transitions with the aim to identify the transitions responsible for the resonant emission at 51.5 eV. This analysis relies on decomposition of time-dependent acceleration $a(t)$ [7] (whose power spectrum is understood to be the HH spectrum) as,

$$a(t) = \sum_{\mu,\nu} \langle \mu | \mathscr{a} | \nu \rangle \, D_\mu^\nu \tag{1}$$

with $\mathscr{a}(\mathbf{r}) = -Z\frac{\cos\theta}{r^2}$, $D_\mu^\nu = \langle \nu | \hat{\rho} | \mu \rangle$, and

$$\rho(\mathbf{r}, \mathbf{r}') = \int \mathrm{d}\sigma_1 \int \mathrm{d}x_2 \ldots \mathrm{d}x_N \, \Psi(\mathbf{r}\sigma_1, x_2, \ldots, x_N)\Psi^*(\mathbf{r}'\sigma_1, x_2, \ldots, x_N).$$

where $|\mu\rangle$ is an initial orbital, Z the nuclear charge, and $\rho(\mathbf{r}, \mathbf{r}')$ is referred to as one particle reduced density matrix (1RDM). From the expression of $\mathscr{a}(\mathbf{r})$, we see that the angular part of matrix element $\langle \mu | \mathscr{a} | \nu \rangle$ obeys the usual dipole selection rules. Therefore, omitting the terms that couple the same orbitals which often vanish if the orbital has a definite angular momentum, one may view the quantity $\alpha(\mu, \nu, t) = 2\,\mathrm{Re}\left\{ \langle \mu | \mathscr{a} | \nu \rangle \, D_\mu^\nu \right\}$ as the contribution from $\mu \leftrightarrow \nu$ orbital transition to the total HHG.

Employing orbital transition-based analysis introduced in the preceding paragraph, we run simulations with a laser having 3×10^{14} W/cm^2 intensity, 770 nm wavelength, and 4-cycle pulse duration on Mn and Mn^+ using TD-ORMAS single-double method with orbital decompositions shown in Fig. 3(a) and (b), respectively. Regarding the method, TD-ORMAS differs from TD-CASSCF in the presence of multiple active spaces (for instance, two active spaces in Fig. 3(a) and (b)) to each of which a restriction on the range of occupation is assigned. In single-double (SD) type, only up to two electrons can occupay Active2 active space. The resulting HH spectra (green) are shown in Fig. 3(c) and (d) along with excita-

tion spectra (purple) of each ionic species. The resonant enhancement around 50 eV is again faithfully reproduced in the HH spectra, at the same energy one can also see a giant transition amplitude in the excitation spectra.

The most important results of our transition analysis are summarized in Fig. 3(e) and (f) where the total spectra (cyan) of all dipole-allowed $3p \leftrightarrow 3d$ transitions, i.e. $\sum_{m=0,\pm1} \alpha(3p_m, 3d_m, t)$, in Mn and Mn^+ are seen to exhibit a prominent peak at 51.5 eV. The total spectra of all transitions among the initial orbitals are also plotted in Fig. 3(e) and (f) in purple. The enhanced peak at 51.5 eV in the total $3p \leftrightarrow 3d$ transition spectrum perfectly coincides with that in the all-transition total spectrum in each ionic species. More importantly, one may also compare the shape of the peaks at and around the resonant energy between all-transition total spectrum and the HH spectrum for each ionic species (Fig. 3(c) and (d)), they are seen to be in a very good agreement as well. This signifies that the emission around the resonant energy is exclusively driven by a coherent electronic dynamics occurring between $3p$ and $3d$ orbitals. In this sense, the enhancement may then be viewed as being the result of a constructive superposition among transition components between the pair of orbitals coupled in resonance.

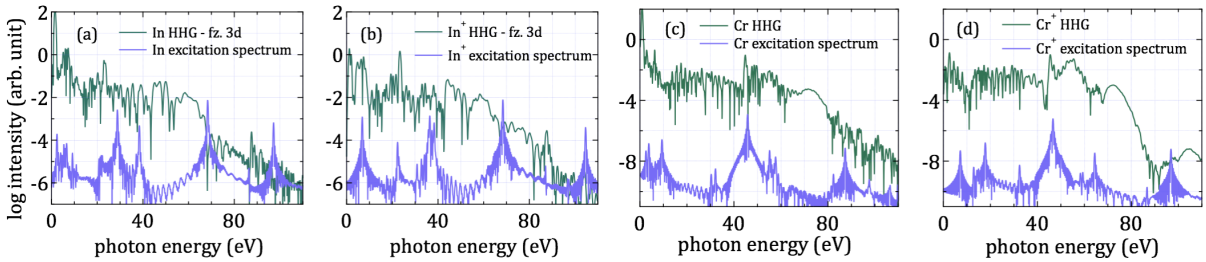

Figure 4: Calculated HH (dark green) and excitation (purple) spectra from (a) In, (b) In^+, (c) Cr, and (d) Cr^+.

Apart from manganese and its cations, we have also applied our *ab initio* methods on indium and chromium plasma. The resulting HH and excitation spectra are shown in Fig. 4. As can be seen, the enhancement in In and In^+ occurs at 23.3 eV whereas in Cr and Cr^+ at 45 eV, excellently confirming the experimental observation (see Fig. 1(a) and (b)).

To conclude, using TD-CASSCF and TD-ORMAS, we have successfully reproduced resonant enhancement in Mn, Mn^+, and Mn^{2+} at an energy close to the experimental value (~ 50 eV) and subsequently, identified the responsible mechanism of the enhancement to be the constructively interfering $3p \leftrightarrow 3d$ transitions. The same methods have also been applied on indium and chromium plasmas for which the enhancement are observed at an energy close to the experimental value, 23.3 eV and 45 eV respectively. These results, to the best of our knowledge, represent a pioneering conclusive work within the subject of resonant HHG from transition metals. With a continuous experimental developement in this field, a coherent, quasi-monochromatic table-top XUV sources based on resonant HHG might be within reach and a precise theoretical description that is in good keeping with this advancement is indispensable.

References

[1] R. A. Ganeev, M. Suzuki, M. Baba, H. Kuroda, and T. Ozaki, Opt. Lett. **31**, 1699 (2006).

[2] R. A. Ganeev, T. Witting, C. Hutchison, F. Frank, M. Tudorovskaya, M. Lein, W. A. Okell, A. Zaïr, J. P. Marangos, and J. W. G. Tisch, Opt. Express **20**, 25239 (2012).

[3] R. A. Ganeev, L. B. E. Bom, J.-C. Kieffer, and T. Ozaki, Phys. Rev. A **75**, 063806 (2007).

[4] T. Sato and K. L. Ishikawa, Phys. Rev. A **88**, 023402 (2013).

[5] T. Sato, K. L. Ishikawa, I. B řezinová, F. Lackner, S. Nagele, and J. Burgdörfer, Phys. Rev. A **94**, 023405 (2016).

[6] T. Sato and K. L. Ishikawa, Phys. Rev. A **91**, 023417 (2015).

[7] I. S. Wahyutama, T. Sato, and K. L. Ishikawa, Phys. Rev. A **99**, 063420 (2019).